



Rheological Behaviors of Lactose Hydrolyzed and Unhydrolyzed Skim Milk Concentrates and Reconstituted Powder Samples

Jessica A. Uhrin¹ · Soraya Shafiekhani¹ · Syed S. H. Rizvi¹

Received: 15 December 2023 / Accepted: 20 March 2024

This is a U.S. Government work and not under copyright protection in the US; foreign copyright protection may apply 2024

Abstract

Lactose hydrolyzed skim milk powder has the potential to become a staple value-added ingredient in snack and frozen foods because 70% of the population suffers from lactose intolerance. However, the flow behavior of lactose hydrolyzed skim milk concentrates and their resulting products need to be understood. The aim of this study was to compare two rheological modeling methods and determine which method is best for predicting rheological behavior in lactose hydrolyzed and unhydrolyzed skim milk concentrates and reconstituted powder samples. The two methods compared are the combined temperature-concentration multiple-linear regression model and the shear rate-temperature-concentration superposition principle master curve model. Prior to fitting the data to the two models, the effect of temperature was determined via the Arrhenius relationship and the effect of concentration was determined via the Exponential relationship. The combined temperature-concentration method resulted in a single logarithmic model for each concentrate type which yields the consistency coefficient at any temperature and concentration input. The master curve method resulted in a single Power law type model for each concentrate type that describes the overall rheological behavior of the samples. When the predicted consistency coefficients from each method were compared to the raw data, both the master curve ($r=0.973$, $P<0.0001$) and the combined ($r=0.940$, $P<0.0001$) methods showed a strong correlation to the raw data. When the results were examined by concentrate type, the master curve model had a stronger fit ($P<0.01$) for the reconstituted samples compared to the combined model which did not show a statistically significant correlation to the raw data ($P<0.075$). The results of this study indicate that the master curve method is superior for predicting the rheological behavior of concentrated milk samples prepared from varying methods within our tested ranges.

Keywords Lactose hydrolyzed skim milk · Viscosity · Skim milk concentrate · Reconstituted lactose hydrolyzed skim milk concentrate · Power law model · Arrhenius model · Master curve

Highlights

- Rheological behaviors of lactose hydrolyzed and unhydrolyzed skim milk concentrates.
- Studied concentrations (10–40% solids) and temperatures (10–40 °C).
- The combined effect of temperature and concentration on the rheological behaviors of LSHM-C, SM-C, LHSM-P, and SM-P was determined.
- Master curves of shear stress versus shear rate/temperature shift factor/concentration shift factor for LSHM-C, SM-C, LHSM-P, and SM-P.
- The superposition modeling method showed stronger correlation values to the raw data compared to the combined effect modeling.

✉ Jessica A. Uhrin
jau25@cornell.edu

¹ Institute of Food Science, Cornell University, Ithaca, NY 14853, USA

Introduction

The production of dairy milk in surplus seasons surpasses the demand; therefore, several methods have been used to store or enhance the shelf life of milk. The most widely used method for extending the shelf life of milk is by converting it into skim milk powder (SMP) which can simply be reconstituted to make traditional dairy products to be used in soups, sauces, and bakery and frozen products. There has been little effort in expanding the utilization of SMP in novel value-added products due to the limitation of its high lactose content (40% lactose) because 70% of the world is lactose intolerant (Ugidos-Rodríguez et al., 2018). As a result of this, milk consumption has dropped by 40% since 1975 (Houssard et al., 2021; Stewart, 2018). This drop in consumption indicates that the current methods for handling

surplus SMP are not enough for an economically sustainable system. In response to this, lactose hydrolyzed skim milk powders are growing in popularity for generating value-added products outside of just the dairy industry. The lactose hydrolyzed and unhydrolyzed skim milk concentrates can be used to make products such as protein-rich extrudates, ice cream, or other snack products that are nutrient-rich and desirable to consumers; thus, the rheological properties of these materials need to be understood.

Lactose hydrolyzed and unhydrolyzed skim milk concentrates are a great value-added ingredient in products because they are rich in highly bioavailable protein as well as vitamins and minerals such as vitamin D, vitamin A, B vitamins, calcium, and potassium (Foroutan et al., 2019). Skim milk concentrate can be made by various methods, including evaporation, reconstitution, membrane filtration, and freeze concentrating. Evaporation is currently the most widely used concentrating method because it yields the highest percent solids values at the lowest cost (Sánchez et al., 2011). This process can be used to prepare skim milk concentrates (of about 40% solids) to be further concentrated into a powder. While skim milk concentrates containing lactose have been well studied, and lactose hydrolyzed skim milk powder has been briefly looked at, there is a gap in knowledge on how lactose hydrolyzed skim milk concentrates rheological behavior (Torres et al., 2017; Vélez-Ruiz & Barbosa-Cánovas, 1998). The flow behavior of skim milk is mainly influenced by casein micelles but is also dependent on time, temperature, and percent solids concentration in the skim milk (da Silva et al. 2017).

Since the flow behavior of milk is strongly influenced by the temperature, the Arrhenius relationship is often used to describe the consistency coefficient in the shear stress vs shear rate model of milk (Abdullah et al., 2018; Deswal et al., 2014; Quek et al., 2013; Rao et al., 1981; Simuang et al., 2004; van Gorp & Palmen, 1998; Vélez-Ruiz & Barbosa-Cánovas, 1998). This relationship can be used to estimate the temperature dependency on the rheological behavior of the lactose-hydrolyzed skim milk concentrates (LHSM-C) and reconstitutes from powder (LHSM-P) compared to skim milk concentrates (SM-C) and reconstitutes from powder (SM-P). Flow behavior is also strongly influenced by the concentration of solids in the system (Rao, 2007). The effect of concentration on the consistency coefficient of skim milk can be described well by either an Exponential Model or a Power law type model (Abdullah et al., 2018; Ahmed, 2017; Kobus et al., 2019; Quek et al., 2013; Rao et al., 1981; van Gorp & Palmen, 1998). The development of a master curve (fitted to a Power law model) can allow for the understanding of the overall flow behavior of lactose hydrolyzed skim milk concentrates and reconstitutes from powder (Anderson et al., 2002; Dak et al., 2007; Harper & Sahrighi, 1965). The master curve is based on the

principle of determining shift factors which can allow for the time–temperature superposition of data (Ahmed, 2017). This technique can also be used to model the effect of temperature and concentration on a variety of liquid concentrates, specifically to this study, to compare the rheological data of concentrates made from lactose hydrolyzed and unhydrolyzed skim milk concentrates and reconstitutes from powders.

The goal of this study was to investigate the influence of concentration (total solids) and temperature on the rheological behaviors of lactose hydrolyzed and skim milk concentrates and reconstitutes from powders. Moreover, two rheological modeling methods (the combined temperature-concentration model and the master curve model) were compared to predict the rheological behavior of these lactose hydrolyzed and unhydrolyzed skim milk concentrates and reconstitutes from powders.

Materials and Methods

Materials

The skim milk (10% solids), lactose-hydrolyzed skim milk (10% solids), and skim milk powder were purchased from the local market of Ithaca, NY, while the lactose-hydrolyzed skim milk powder was obtained from Valio Ltd. (Helsinki, Finland).

Preparation of Milk Concentrates and Reconstitutes

The skim milk concentrate (SM-C) and lactose-hydrolyzed skim milk concentrate (LHSM-C) were made by concentrating the skim milk and lactose-hydrolyzed skim milk, respectively, to 40% total solid using a 50 L Rotary Evaporator (50L BVV™ ECO Rotary Evaporator, Napperville, IL). The Rotary Evaporator was used at a pressure of 30 inHg and temperature of 48 °C to avoid Maillard browning in the milk during evaporation. These SM-C and LHSM-C concentrates (having 40% solids) were further diluted with deionized water to 30% and 20% total solids. Similarly, skim milk powder and lactose-hydrolyzed skim milk powders were reconstituted with water to make 10, 20, 30, and 40% solid concentrations. These reconstituted skim milk concentrate (SM-P) and lactose-hydrolyzed skim milk concentrate (LHSM-P) were allowed to sit overnight for complete hydration under refrigeration (4 °C). The total solids contents of the above samples were verified by AOAC (2005).

Rheological Measurements

The rheology of LHSM-C, SM-C, LHSM-P, and SM-P concentrates was studied by using a rheometer (Rheolyst AR 1000-N, TA Instruments, New Castle, DE, USA). The rheometer was fitted with a 6-cm, 2° steel cone with a flat

Peltier plate base configured with a cone-plate geometry. Small portions of samples were placed between the cone and plate and the distance between the plate was set to 78 μm . Samples were tested under continuous shear rate flow ramps, with shear rates between 0 and 1000 $1/\text{s}$ at temperatures of 10, 20, 30, and 40 $^{\circ}\text{C}$. All tests were done in triplicate.

Effect of Temperature, Concentration, and Combined Effect of Temperature and Concentration on Rheological Behavior

The effect of temperature on the consistency coefficient (K) was determined by an Arrhenius relationship:

$$K = K_0 \exp\left(\frac{E_a}{RT}\right) \quad (1)$$

where K is the consistency coefficient, K_0 is the pre-exponential factor, E_a (kJ/mol) is the activation energy, R (J/mol) is the gas rate constant, and T ($^{\circ}\text{C}$) is the temperature. The linearized form of Eq. 1 (Quek et al., 2013) was plotted to determine y -intercept or the pre-exponential factor, K_0 (Pa s^n). The activation energy, E_a (kJ/mol), was determined by multiplying the slope by the gas constant.

The Power law (Eq. 2) and Exponential (Eq. 3) models were used to determine the effect of concentration (% solids) on the consistency coefficient, K (Pa s^n).

$$K = K_1 C^{n_1} \quad (2)$$

$$K = K_2 \exp(n_2 C) \quad (3)$$

The consistency constants (K_1 and K_2) and flow behavior constants (n_1 and n_2) were determined by Eqs. 2 and 3 (Abdullah et al., 2018; Kobus et al., 2019; Quek et al., 2013) at the four tested temperatures and four concentrations.

The combined effect of both temperature and concentration on the consistency coefficient was determined by combining the Arrhenius and Exponential models into a single logarithmic model (Vélez-Ruiz & Barbosa-Cánovas, 1997):

$$\ln(K) = \beta_0 + \beta_1 \left(\frac{1}{T}\right) + \beta_2 C \quad (4)$$

Equation 4 was used to determine the consistency coefficient, K (Pa s^n), and activation energy, E_a (kJ/mol), from the combined effect of temperature, T ($^{\circ}\text{C}$), and concentration, C (% solids). The magnitudes of the coefficients (β_1 and β_2) were estimated by a multiple linear regression analysis of the natural logarithm of the consistency coefficient (K), percent concentration (C), and absolute temperature (T) data (Vélez-Ruiz & Barbosa-Cánovas, 1997) done using JMP Pro 16 (SAS Institute Inc., Cary, N.C.). β_1 represents the temperature dependency of the consistency coefficient and is equal to E_a/R from the Arrhenius model. β_2 represents the

concentration dependency of the consistency coefficient and is equal to n_2 from the Exponential model and β_0 represents the intercept. Therefore, Eq. 4 can be written as follows:

$$K = \exp\left(\beta_0 + \frac{E_a}{R} \left(\frac{1}{T}\right) + n_2 C\right) \quad (5)$$

Modeling Fluid Flow at Different Temperatures and Concentrations

A total of 64 flow curves resulted from testing the rheological behaviors of the four milk concentrates at different temperatures (10, 20, 30, and 40 $^{\circ}\text{C}$) and concentrations (10, 20, 30, and 40% solids). These 64 average flow curves (16 per sample) were combined by using the superposition technique to form a master curve to consolidate all the information gathered into a single usable graphic. The superposition technique requires the data to be shifted towards set reference points; for the purpose of this study, a reference temperature of 20 $^{\circ}\text{C}$ (close to room temp) and a shear stress basis of 1 Pa (a low shear stress) were selected. The other three temperatures (10, 30, and 40 $^{\circ}\text{C}$) at common concentration were shifted horizontally along the shear rate axis to the reference temperature of 20 $^{\circ}\text{C}$ to obtain the dimensionless shear rate-temperature shift factors, a_T , defined as the ratio of shear rate at other temperature at basis shear stress (1 Pa) to the shear rate at the reference temperature (20 $^{\circ}\text{C}$) as shown in Eq. 6.

$$a_T = \frac{\dot{\gamma}}{\dot{\gamma}_R} \quad (6)$$

The first shift reduces the 64 flow curves into 16 master curves (4 for each sample/4 master plots) which were plotted as shear stress versus shear rate divided by the dimensionless shift factor. Power law equation (Eq. 7) was then fitted to the four concentration master curves to obtain the expression of rheological behavior of different milk concentrates (SM-C, LHSM-C, SM-P, and LHSM-P) in terms of consistency coefficient, K' , and flow behavior index, n' .

$$\sigma = K' \left(\frac{\dot{\gamma}}{a_T}\right)^{n'} \quad (7)$$

The second shifting step is used to determine the concentration shift factor. The four concentration master curves for each milk concentrates (SM-C, LHSM-C, SM-P, and LHSM-P) were shifted to a reference concentration of 30% (the concentration of interest for future work) at a shear stress basis of 1 Pa to make a single final master curve using the concentration shift factor of a_C . The final master curve for each sample was plotted as shear stress versus shear rate divided by the temperature and concentration shift factors to

estimate the rheological behavior of each concentrated milk (SM-C, LHSM-C, SM-P, and LHSM-P) at concentration of 10–40% and temperature of 10–40 °C. The final master curve expression (Eq. 8) simply and concisely describes the rheological behavior of milk concentrates (SM-C, LHSM-C, SM-P, and LHSM-P) in terms of consistency coefficient, K'' , and flow behavior index, n'' .

$$\sigma = K'' \left(\frac{\dot{\gamma}}{a_T \times a_C} \right)^{n''} \quad (8)$$

Statistical Analysis

All experiments were conducted at least three times and their results were shown as mean \pm standard deviation (SD). Statistical significance was calculated through a one-way analysis of variance (P -values < 0.05) and post hoc Tukey adjustment using JMP Pro 16 (SAS Institute Inc., Cary, N.C.). Figures created in RStudio using ggplot2 (Hadley, 2016).

Results and Discussion

Effect of Temperature on Rheological Behavior

Table 1 shows the effect of temperature (10, 20, 30, and 40 °C) on rheological behavior of samples (LHSM-C, SM-C, SM-P and LHSM-P) at different concentrations of 10, 20, 30, and 40%. The resulting parameters of the Arrhenius relationship (average $R^2 = 0.96 \pm 0.04$) between consistency coefficient and temperature showed that the consistency coefficient in all samples decreased with increasing temperature. Generally, the reconstitute samples (SM-P and LHSM-P) had higher activation energies compared to the evaporated samples (SM-C and LHSM-C) shown in Table 1. The higher the activation energy, the higher the sensitivity of the viscosity to temperature (Kaya & Sozer, 2005). Results showed that the average activation energy of the LHSM-P-40 and SM-P-40 reconstitutes from powder (56.0 ± 15 kJ/mol) was almost two times higher than the activation energy for the two concentrates (LHSM-C and SM-C) made by evaporation (30.8 ± 2.4 kJ/mol); this is likely due to the denaturation of the whey protein and β -LG that occurs in the LHSM-P and SM-P during the high temperature drying process that is required in order to manufacture a milk powder (Anandharamakrishnan et al., 2007) and increases the LHSM-P/SM-P-40's resistance to flow. Moreover, the activation energies associated with temperature dependence of consistency coefficient also increased with concentration (% solids) across all samples. This phenomenon was expected because as the solid

Table 1 Effect of temperature on consistency coefficient, K_0 (Pa sⁿ), and associated activation energy, E_a (kJ/mol), on lactose hydrolyzed (LHSM-C) and unhydrolyzed skim milk concentrates (SM-C) and reconstituted powder samples (LHSM-P and SM-P)

Concentrate type	Concentration (solids %wt)	K_0 (Pa s ⁿ)	E_a (kJ/mol)	R^2
LHSM-C	10.0	9.00E-05	9.90	0.934
	20.0	1.00E-05	16.3	0.980
	30.0	7.00E-07	24.0	0.941
	40.0	4.00E-07	29.1	0.960
SM-C	10.0	9.00E-05	10.2	0.999
	20.0	3.00E+00	20.0	0.980
	30.0	3.00E-06	21.0	0.990
	40.0	6.00E-08	33.0	0.942
LHSM-P	10.0	3.00E-05	14.0	0.844
	20.0	2.00E-06	22.1	0.997
	30.0	1.00E-11	56.0	0.943
	40.0	3.00E-13	66.2	0.999
SM-P	10.0	3.00E-05	13.0	0.975
	20.0	2.00E-06	22.0	0.960
	30.0	9.00E-06	21.3	0.950
	40.0	9.00E-10	46.0	0.927

concentration in the milk increases, it becomes less fluid-like and more solid based and, therefore, more resistant to flow (Zhang et al., 2015). This increase in flow resistance means that the higher solid concentration milk concentrates require a higher initial energy to initiate the particle movement and ultimately the flow of liquid.

The activation energies were within the normal ranges of what others have reported (Dak et al., 2008). One study on concentrated whole milk determined the activation energies for the evaporation concentrated milk between concentrations 12.6 and 42.4% solids (Vélez-Ruiz & Barbosa-Cánovas, 1998). The activation energies this study determined for the whole milk concentrate samples follow the same trend as our results for the lactose hydrolyzed and unhydrolyzed skim milk concentrates, indicating an increase in activation energy with an increase in concentration (% solids).

Another study on tomato concentrate from 8.04 to 18% solid concentration found that the activation energy ranged from 8.6 to 14.08 kJ/mol (Dak et al., 2008) which is fairly similar to the activation energies of this study for 10–20% solids LHSM-C, SM-C, LHSM-P, and SM-P which ranged from 9.90 to 22.1 kJ/mol. For all four milk types, there is a trend of increasing activation energy with increasing solid concentration; this increase in activation energy with concentration was also seen by Solanki and Rizvi (2001); in their study of concentrated skim milk, they reported a 130% increase in activation energy with a three-fold increase in concentration (Solanki & Rizvi, 2001).

This increase in flow resistance was observed across all the concentrations of LHSM-P, although most dramatically in the 30% and 40% solid concentrations; this might be due to the low lactose content available during the LHSM-P drying process (Allison et al., 1999; Baldwin, 2010; Havea, 2006; Prestrelski et al., 1993; Torres et al., 2017). Lactose plays an important role in maintaining protein structure during drying. The lactose can hydrogen bond to the proteins in place of the water molecules that are lost along the hydrophilic outer layer of the casein micelle as the powder is being dried. The lactose can also act as a mechanical spacer to prevent the protein bonding (without this spacer, the casein micelles form weak hydrophobic non-covalent bonds with each other which decrease their solubility). Also, once bound to the amino acid chain, the lactose will act as a hydrophilic pathway to transfer moisture to the micelle during rehydration. Since the LHSM-P would be lacking this protective lactose, therefore, it would have poor rehydration characteristics (Allison et al., 1999; Baldwin, 2010; Havea, 2006; Prestrelski et al., 1993; Torres et al., 2017). It is also important to note that this mechanical spacer behavior is not seen in glucose and galactose (Allison et al., 1999).

In the SM-P, the increase in flow resistance is most noticeable in the 40% solids concentration, while in the 10–30% solid concentrations, the flow resistance behavior of the SM-P is more like the samples made through evaporation (SM-C and LHSM-C). This drastic increase in activation energy that makes the SM-P-40 more similar to the LHSM-P-40 is likely due to the concentration of coagulated proteins having exceeded a certain threshold value at which the coagulation exponentially increases the resistance to

flow (Dahbi et al., 2010). The temperature dependence of the concentrates and reconstitutes showed increasing resistance to flow with increasing concentration (% solids), as would be expected, but the reconstitute samples had an overall higher activation energy than the concentrate samples suggesting the powder processing results in a reconstitute with a higher resistance to flow at the same concentration as a concentrate made by evaporation. Moreover, the LHSM-P sample had a higher activation energy than the SM-P sample indicating that the lactose content, or lack thereof, also plays a significant role in the resulting resistance to flow of the reconstitutes from powder.

Effect of Concentration on Rheological Behavior

To determine whether the consistency coefficient increased logarithmically or exponentially with concentration, the consistency coefficient of the different concentrates was fitted to both a Power law model and an Exponential model as a function of concentration. The resulting K constants (K_1 and K_2) and n constants (n_1 and n_2) for all four of the different milk concentration types are shown in Table 2. For LHSM-C and SM-C, as the temperature increased, K_1 increased, K_2 decreased, and n_1 and n_2 decreased. For LHSM-P and SM-P, as the temperature increased, K_1 and K_2 increased and n_1 and n_2 decreased. While the Power law model was a good fit (average $R^2 = 0.86 \pm 0.09$) for all the concentrate types, the Exponential model exhibited a slightly better fit (average $R^2 = 0.92 \pm 0.05$) indicating the consistency coefficient increased exponentially with concentration. The increase in total solids could increase the interactions among casein

Table 2 Effect of concentration on consistency coefficient on lactose hydrolyzed (LHSM-C) and unhydrolyzed skim milk concentrates (SM-C) and reconstituted powder samples (LHSM-P and SM-P) fitted to Power law model variables K_1 and n_1 and Exponential model variables K_2 and n_2

Concentrate type	Temperature (°C)	K_1	n_1	R^2	K_2	n_2	R^2
LSM-C	10.0	8.00E-05	1.80	0.820	2.10E-03	0.088	0.944
	20.0	1.00E-04	1.50	0.780	2.00E-03	0.074	0.921
	30.0	2.00E-04	1.24	0.717	2.00E-03	0.063	0.880
	40.0	2.00E-04	1.23	0.740	1.80E-03	0.062	0.893
SM-C	10.0	3.00E-04	1.32	0.860	3.70E-03	0.063	0.944
	20.0	3.00E-04	1.22	0.800	3.00E-03	0.060	0.921
	30.0	5.00E-04	0.950	0.804	3.10E-03	0.046	0.920
	40.0	7.00E-04	0.770	0.890	3.10E-03	0.036	0.950
LHSM-P	10.0	3.00E-06	3.30	0.790	1.50E-03	0.151	0.890
	20.0	4.00E-05	2.50	0.940	2.00E-03	0.111	0.998
	30.0	1.00E-04	2.00	0.960	2.00E-03	0.094	0.892
	40.0	3.00E-13	1.50	0.964	2.20E-03	0.070	0.950
SM-P	10.0	9.00E-06	2.73	0.970	1.50E-03	0.131	0.998
	20.0	3.00E-05	2.13	0.970	1.90E-03	0.100	0.900
	30.0	4.00E-05	1.93	0.960	1.70E-03	0.092	0.900
	40.0	4.00E-04	1.93	0.890	1.50E-03	0.090	0.780

K_1 and K_2 are consistency coefficient constants, while n_1 and n_2 are flow behavior constants

micelles, whey proteins, and carbohydrates (either lactose or glucose and galactose). This increase in bonding behavior results in an increase in viscosity which is shown by the trend of increasing consistency coefficients and decreasing flow behavior indices in all the milk concentrates.

Combined Effect of Temperature and Concentration on Rheological Behavior

The combined effect of concentration and temperature on the consistency coefficient of the samples was examined using a single logarithmic model for simulation purposes. Figure 1 shows the two separate independent variables' (temperature and concentration) influence on the consistency coefficient. Table 3 shows the magnitudes of the β coefficients for the combined model. The R^2 value of the equations for each concentrate type suggests good fit to the experimental data obtained. The root mean square error (RMSE) values for the

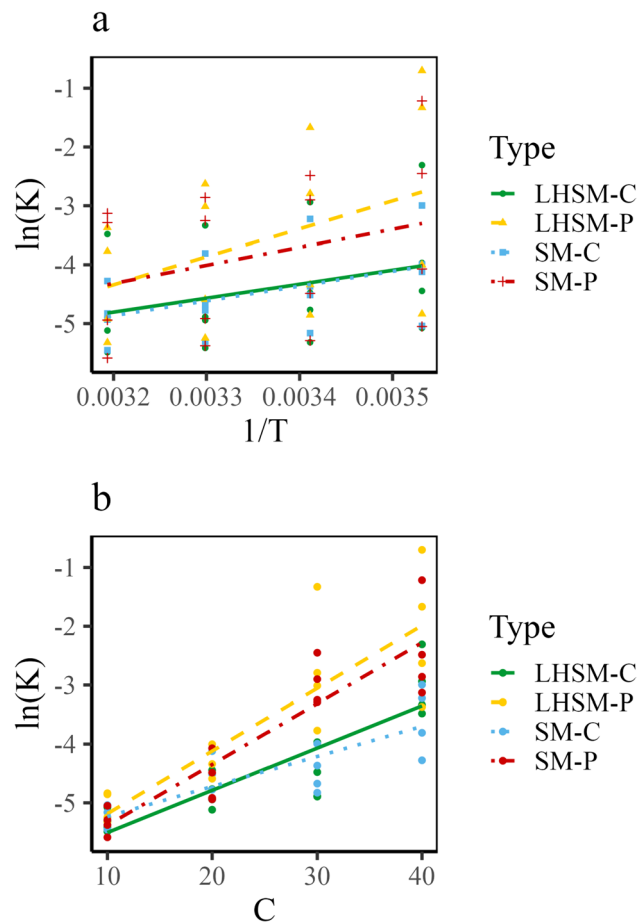


Fig. 1 Effect of **a** absolute temperature, $1/T$ (K), and **b** concentration, C (% solids), on consistency coefficient, K (Pa s.ⁿ), using the Combined effect model (Eq. 4) for lactose hydrolyzed (LHSM-C) and unhydrolyzed skim milk concentrates (SM-C) and reconstituted powder samples (LHSM-P and SM-P)

Table 3 Constant values for the combined effect of temperature and concentration on the consistency coefficient of lactose hydrolyzed (LHSM-C) and unhydrolyzed skim milk concentrates (SM-C) and reconstituted powder samples (LHSM-P and SM-P)

Concentrate type	β_0	β_1	β_2	R^2	Mean E_a
LHSM-C	-14.2	2370	0.071	0.870	20.0
SM-C	-14.2	2510	0.051	0.910	21.0
LHSM-P	-22.2	4747	0.110	0.902	43.4
SM-P	-17.0	3064	0.103	0.934	38.0

β_1 and β_2 are coefficients estimated by a multiple linear regression analysis of the natural logarithm of the consistency coefficient (K), percent concentration (C), and absolute temperature (T) data. β_1 represents the temperature dependency of the consistency coefficient and is equal to E_a/R from the Arrhenius model. β_2 represents the concentration dependency of the consistency coefficient and is equal to n_2 from the Exponential model and β_0 represents the intercept

models are 0.363 ± 0.11 indicating the models perform relatively well at predicting the data accurately. This combined effect model allows for the consistency coefficient of the LHSM-C, SM-C, LHSM-P, and SM-P to be determined at any temperature or concentration. Figure 1 indicates that the consistency coefficient increases with both concentration and temperature. Within the combined models, the variable importance was determined. The resulting total effect of the concentration (% solids) and absolute temperature was 0.833 ± 0.10 and 0.170 ± 0.10 , respectively, for the samples indicating the concentration variable has a stronger effect on the resulting consistency coefficient. Therefore, in a processing situation (e.g., extrusion) where the consistency coefficient of the material needs to be controlled within a certain range, the concentration of the lactose hydrolyzed and unhydrolyzed concentrates is the most important variable to consider.

Modeling Fluid Flow Using Master Curve

To understand the overall flow characteristics of the different milk concentrates, a superposition technique was used to generate a master curve of all the samples. In general, the shear stress versus shear rate curves of different milk concentrate types (LHSM-C, SM-C, LHSM-P, and SM-P) at different temperatures (10, 20, 30, and 40 °C) and concentrations (10, 20, 30, and 40%) had a similar pattern (indicated in Table 1 and 2); the shear stress curves could be shifted horizontally along the shear rates axis to a reference temperature of 20 °C. A shear stress basis of 1 Pa was used for obtaining the shift factor to make a master curve. The values of shear rate-temperature shift factors ($a_T = \dot{\gamma}/\dot{\gamma}_R$) for milk concentrates (SM-C, LHSM-C, SM-P, and LHSM-P) curves are presented in Table 4. The shift factors at reference temperature of 20 °C curves are equal to 1. The shifted data can be seen in Fig. 2. The parameters of consistency coefficient and flow behavior index, obtained by fitting the

Table 4 Temperature and concentration shift factors a_T and a_C used to generate the master curves for lactose hydrolyzed (LHSM-C) and unhydrolyzed skim milk concentrates (SM-C) and reconstituted powder samples (LHSM-P and SM-P)

Concentrate type	Concentration (solids %wt)	a_T				a_C
		Temperature (°C)				
		10	20	30	40	
LHSM-C	10.0	0.984	1.00	1.12	1.20	1.60
	20.0	0.684	1.00	1.21	1.30	1.61
	30.0	0.581	1.00	1.02	2.30	1.00
	40.0	0.490	1.00	1.50	1.83	0.25
SM-C	10.0	0.790	1.00	1.10	1.10	2.12
	20.0	0.670	1.00	1.40	1.70	1.10
	30.0	0.630	1.00	1.30	1.50	1.00
	40.0	0.860	1.00	2.31	3.32	0.31
LHSM-P	10.0	0.920	1.00	1.23	1.24	15.0
	20.0	0.672	1.00	1.40	1.60	8.23
	30.0	0.210	1.00	2.90	5.74	1.00
	40.0	0.102	1.00	4.90	13.0	0.42
SM-P	10.0	1.040	1.00	0.85	0.98	10.1
	20.0	0.660	1.00	1.20	2.00	4.80
	30.0	0.260	1.00	1.33	1.40	1.00
	40.0	0.150	1.00	1.64	2.40	0.80

single shifted master curves to a Power law model, are presented in Table 5 with R^2 . Overall, the consistency coefficient increases, and the flow behavior index decreases with the increase in concentration indicating the LHSM-C, SM-C, LHSM-P, and SM-P concentrates exhibited an increase in consistency coefficient and shear thinning with an increase in solids concentration.

The three concentration master curves at 10, 20, and 40% were then shifted to a reference concentration of 30% at a shear stress basis of 1 Pa. Single final master curves describing the rheological behavior of each milk concentrate types (SM-C, LHSM-C, SM-P, and LHSM-P) are shown in Fig. 3 (shifted raw data shown in Fig. 2). The values of shear rate-concentration shift factors (a_C) as a second reduced shear rate ($a_C = \dot{\gamma}_R / \dot{\gamma}''$) are presented in Table 4. The final master curve for each concentrate type was then fitted into a Power law equation to determine the relationship between shear stress, shear rate, consistency coefficient, and flow behavior index and yielded Table 6 (Eqs. 8–11).

This second shift allowed for the formation of a final master curve (Fig. 3) for each milk concentrate type which can be used to describe the flow behavior and predict how each milk concentrate type will behave in different processing situations. The superposition method extends the shear rate range with respect to shear stress as a function of the temperature and concentration shift factors; therefore, the $\dot{\gamma}''$ (shear rate/ a_T/a_C) range is wider than the tested range. The concentrated from liquid samples (LHSM-C and SM-C) show a more Newtonian behavior with flow behavior index values of 0.882 and 0.831 (Eqs. 8 and 9 in Table 6), respectively,

and straight fit lines in Fig. 3. The reconstituted from powder samples (LHSM-P and SM-P) show a non-Newtonian shear thinning behavior indicated by flow behavior index values of 0.714 and 0.792 (Eqs. 10 and 11 in Table 6), respectively, and concave fit lines in Fig. 2.

The max shear stress for each sample occurred at concentration 40% solids, temperature 10 °C, and at a shear rate of 1000 (1/s). The resulting master curve max shear stress for LHSM-P, SM-P, LHSM-C, and SM-C was 92.0, 41.0, 30.1, and 17.0, respectively. Figure 3 shows the master curves for all the samples up to a temperature and concentration shift factor converted shear rate of 3000 (1/s). The max shear stress point, shown outside the ranges of Fig. 3 (data can be found in supplemental), indicates that the unhydrolyzed samples have a lower shear stress with respect to shear rate, concentration, and temperature, while the hydrolyzed samples exhibited higher max shear stress points.

When comparing the master curve equations themselves (Eqs. 9–12 in Table 6), the consistency coefficients for the reconstituted from powder samples σ_{LHSM-P} ($K=0.148$) and σ_{SM-P} ($K=0.0706$) were higher than the concentrates from liquid samples σ_{LHSM-C} ($K=0.0146$) and σ_{SM-C} ($K=0.0193$). The σ_{LHSM-P} ($K=0.148$) consistency coefficient was about double the σ_{SM-P} ($K=0.0706$) consistency coefficient, indicating that the consistency coefficient for the LHSM-P sample is more sensitive to changes in concentration and temperature.

This drastic increase in consistency coefficient in the reconstitutes might be due to the processing conditions for the LHSM-P and to an extent the SM-P which includes heating the powder to high temperatures above 80 °C via

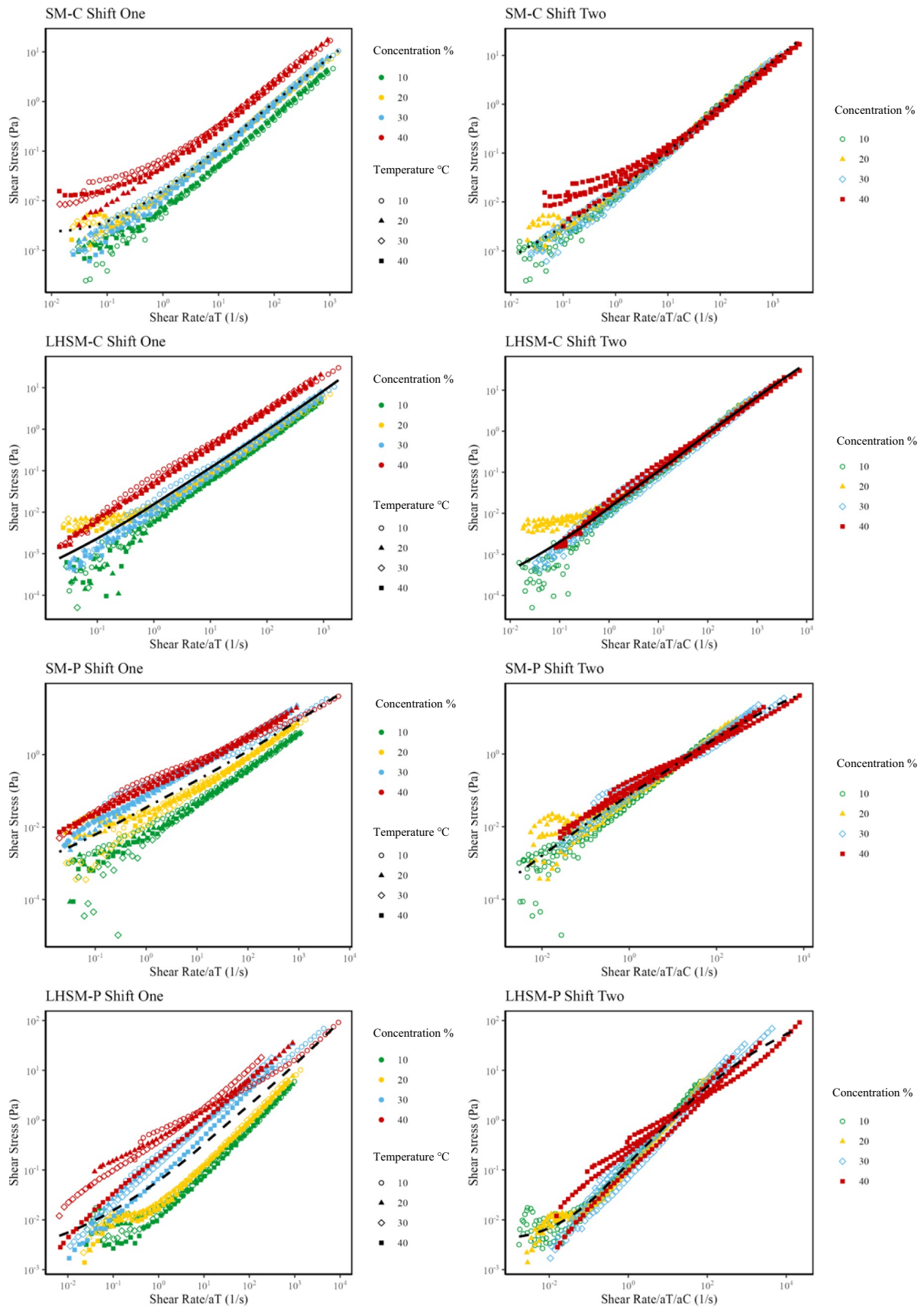


Fig. 2 Shear rate values for lactose hydrolyzed (LHSM-C) and unhydrolyzed skim milk concentrates (SM-C) and reconstituted powder samples (LHSM-P and SM-P) were shifted first by temperature, °C (shift one), then by concentration, % solids (shift two)

spray drying, which could denature the whey proteins causing the product to thicken at higher concentrations (around 40% solids). During spray drying (80–120 °C) or heating the milk above 65 °C, the globular proteins unfold and reassociate to form aggregates; the whey proteins α -lactalbumin (α -LA) and β -lactoglobulin (β -LG) are the specific globular proteins that experience this unfolding and formation of protein aggregates with casein (Zhao et al., 2020). Of these whey proteins, β -LG has a more significant impact on the flow behaviors of the reconstituted milk (Anandharamakrishnan et al., 2008). The β -LG has two disulfide bonds and one free thiol group which are responsible for the aggregation and gelling properties of the β -LG (Joyce et al., 2017). When heated, k-casein (k-CN) dissociates from the casein micelle and forms a complex with the β -LG; further heating causes a decrease in pH (Zhao et al., 2020). These chemical changes were most pronounced in the reconstitutes as they had the highest amount of heat treatment, through both pasteurization and spray drying. Even though there were differences in the flow behaviors at the higher percent solids concentrations, the different concentrate types (LHSM-C, SM-C, LHSM-P, SM-P) still showed a similar consistency coefficient dependence on temperature.

Table 5 Parameters of Power law fitting to shear rate/temperature master curve data of lactose hydrolyzed (LHSM-C) and unhydrolyzed skim milk concentrates (SM-C) and reconstituted powder samples (LHSM-P and SM-P)

Concentrate type	Concentration (solids %wt)	Consistency coefficient, K'	Flow behavior index, n'	R^2
LHSM-C	10.0	0.010	0.990	0.998
	20.0	0.022	0.731	0.980
	30.0	0.012	0.923	0.981
	40.0	0.051	0.880	0.990
SM-C	10.0	0.010	0.880	0.992
	20.0	0.020	0.822	0.992
	30.0	0.020	0.872	0.994
	40.0	0.080	0.720	0.983
LHSM-P	10.0	0.024	0.700	0.970
	20.0	0.031	0.731	0.983
	30.0	0.120	0.802	0.960
	40.0	0.320	0.644	0.952
SM-P	10.0	0.010	0.902	0.990
	20.0	0.080	0.770	0.921
	30.0	0.030	0.750	0.984
	40.0	0.130	0.690	0.953

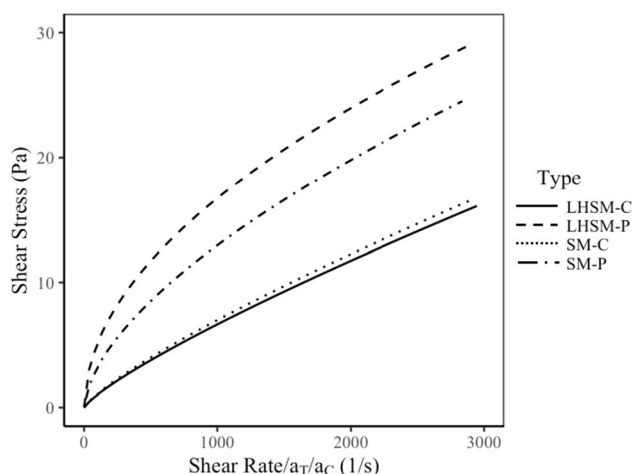


Fig. 3 Master curves of shear stress versus converted shear rate/temperature/concentration shift factors axis of lactose hydrolyzed (LHSM-C) and unhydrolyzed skim milk concentrates (SM-C) and reconstituted powder samples (LHSM-P and SM-P)

Alternatively, the increased consistency coefficient of the LHSM-P samples—especially when compared to the SM-P samples—might be due to the increased wetting time of the LHSM-P powder. Decreased wettability or dissolvability of milk powders leads to an increased consistency coefficient. In high concentrations of milk powders (reconstituted into concentrates), the protein and lactose content become very important variables to determine the solubility and consistency coefficient of the milk powders (Warncke & Kulozik, 2020). Casein is the least dissolvable protein in milk powders; lactose helps improve the dissolvability of the milk powder by preventing protein–protein interactions which usually result in protein aggregates. Lactose prevents this by hydrogen bonding to the amino acid chain and acts as a steric spacer (Warncke & Kulozik, 2020). Since the LHSM-P analyzed in this study is first lactose filtered and

Table 6 Final master curve equation for each concentrate type of lactose hydrolyzed (LHSM-C) and unhydrolyzed skim milk concentrates (SM-C) and reconstituted powder samples (LHSM-P and SM-P)

Concentrate type	Master curve equation
LHSM-C	$\sigma_{LHSM-C} = 0.0146 \left(\frac{\dot{\gamma}}{a_T \times a_C} \right)^{0.8819} \quad R^2 = 0.980 \quad (9)$
SM-C	$\sigma_{SM-C} = 0.0193 \left(\frac{\dot{\gamma}}{a_T \times a_C} \right)^{0.8305} \quad R^2 = 0.983 \quad (10)$
LHSM-P	$\sigma_{LHSM-P} = 0.1489 \left(\frac{\dot{\gamma}}{a_T \times a_C} \right)^{0.7142} \quad R^2 = 0.830 \quad (11)$
SM-P	$\sigma_{SM-P} = 0.0706 \left(\frac{\dot{\gamma}}{a_T \times a_C} \right)^{0.7921} \quad R^2 = 0.870 \quad (12)$

σ denotes shear stress, $\frac{\dot{\gamma}}{a_T \times a_C}$ denotes the shear rate shifted by the dimensionless temperature (a_T) and concentration (a_C) shift factors

Table 7 Testing master curve (Eqs. 9, 10, 11, 12) and combined effect prediction models (Eq. 4) of lactose hydrolyzed (LHSM-C) and unhydrolyzed skim milk concentrates (SM-C) and reconstituted powder samples (LHSM-P and SM-P) within the tested ranges

Concentrate type	Method	Pearson's correlation value to experimental consistency coefficient (Pa s ⁿ)	P-value
LHSM-C	Combined	0.950	0.054*
	Master curve	0.990	0.010*
SM-C	Combined	0.962	0.040*
	Master curve	0.998	0.003*
LHSM-P	Combined	0.934	0.070
	Master curve	0.993	0.0071*
SM-P	Combined	0.943	0.060
	Master curve	0.999	0.0011*
Overall	Combined	0.940	<0.0001*
	Master curve	0.973	<0.0001*

P values less than 0.05 were given an asterisk

then hydrolyzed, so there is very little to no lactose available to prevent this aggregation of caseins; therefore, have higher protein content in the LHSM-P than the LHSM-C—according to the manufacturer specifications. Both variables, the processing conditions and lactose content, together resulted in the LHSM-P having a higher consistency coefficient than its LHSM-C, SM-C, and SM-P counterparts.

The difference in consistency coefficient demonstrated by the master curve equations supports the hypothesis that lactose is an important component during the drying process to maintain protein solubility. The σ_{SM-P} has a slightly higher consistency coefficient compared to the samples made via evaporation because the SM-P still goes through spray drying; it just has the high lactose content (SM-P is about 50% lactose) as a protective measure against most of the decreased solubility, and therefore increased consistency coefficient, that is seen in the LHSM-P. The σ_{LHSM-C} and σ_{SM-C} behave similar because these concentrate types have not undergone the spray drying step that the reconstitutes have and therefore have almost identical consistency coefficients and flow behavior indices.

These master curves are also useful in comparing the data of flow behavior from different milk concentrate types during varied application and processing conditions. Rao (2007) described the different shear rates that materials undergo during typical processing conditions such as mixing, pipe flow, spraying, and extrusion. The shear rates given for these processing measures were shear rates between 1 and 100,000 (Rao, 2007), a large portion of which can be seen on the final master curves for each milk concentrate. The shown portion of the master curve model in Fig. 2 shows the shear rate region which extrusion would fall into. Having this tool as a predictive model for the behavior of lactose-free concentrates made via evaporation and reconstitution is a valuable resource for the industry especially since the market for lactose-free products is projected to grow to USD 17.1 billion by 2026 (Market Data Forecast, 2022) indicating large opportunity for novel products (e.g., extruded snacks).

Comparing Master Curve Modeling Method to Combined Modeling Method

The combined and master curve models were validated against the raw data for the consistency coefficient, K (Pa sⁿ). The models were validated at a constant temperature of 30 °C with varying concentrations within the tested range of 10–40 °C with in-between values shown as well to show the strength of each model's estimation capabilities. Table 7 shows the results of testing the models against the raw data for consistency coefficient.

The correlation value (r) for each model to the raw data, shown in Table 7, was determined by fitting the models' predicted coefficient values as a function of the raw data values. Both the combined model and the master curve model fit the raw data consistency coefficient values well with correlation values of $r=0.940$, $P<0.0001$ (combined) and $r=0.973$, $P<0.0001$ (master curve). The master curve model was a slightly better fit with both LHSM-C ($r=0.990$, $P<0.010$) and SM-C ($r=0.998$, $P<0.003$) samples. The master curve correlations for LHSM-P ($r=0.993$, $P<0.008$) and SM-P ($r=0.999$, $P<0.002$) were significantly better than the combined model correlations ($r=0.934$, $P<0.08$ and $r=0.943$, $P<0.07$), respectively. The master curve model has predicted values within the tested range for all sample types that are strongly correlated to the raw data values ($P<0.01$) making it the better model for testing the milk concentrates made either from reconstitution or evaporation.

Conclusion

Aqueous dispersions of 10–40% solids of lactose hydrolyzed and unhydrolyzed skim milk concentrates and reconstitutes were prepared by vacuum evaporation and reconstituted from powder. The effects of temperature and concentration were then combined to create a model that allows for the

determination of the consistency coefficient of all the sample types at any concentration and temperature. The combined temperature-concentration dependence model indicated that concentration had the larger effect on the consistency coefficient, and therefore, it is the most important variable to consider for these samples resulting flow behavior.

The shear rate-temperature-concentration superposition principle was utilized to make a single master curve for each sample type that models the flow behavior of lactose hydrolyzed and unhydrolyzed skim milk concentrates and reconstituted powers within our tested ranges. While the results of this study suggest that either method could be used for determining the consistency coefficients of lactose hydrolyzed and unhydrolyzed skim milk concentrates, the master curve model yields consistency coefficient values that have a stronger correlation to the experimentally determined consistency coefficient indicating the superposition principle is the superior methodology when predicting flow behaviors of LHSM-C, SM-C, LHSM-P, and SM-P. The results of this study are useful for the utilization of hydrolyzed and unhydrolyzed skim milk in a variety of products ranging from bakery and snack products to ice cream and frozen desserts.

Supplementary Information The online version contains supplementary material available at <https://doi.org/10.1007/s11947-024-03386-0>.

Author Contribution Syed S.H. Rizvi - Conceptualization, Supervision, Review & editing, Funding acquisition, Project administration. Jessica A. Uhrin - Data acquisition, Data analysis, Writing, Data Visualization, Review & editing Soraya Shafiekhani - Data analysis, Writing, Review & editing.

Funding This research was supported by the 2021 Dairy Promotion Order, Empire State Development Project no. C013079 and the US Department of Agriculture National Institute of Food and Agriculture, grant: 2020-67017-31192.

Data Availability Datasets available in supplementary section.

Declarations

Competing Interests This research was supported by the 2021 Dairy Promotion Order, Empire State Development Project no. C013079 and the US Department of Agriculture National Institute of Food and Agriculture, grant: 2020-67017-31192.

References

- Abdullah, N., Chin, N. L., Yusof, Y. A., & Talib, R. A. (2018). Modeling of rheological behaviour of guava, pomelo and soursop juice concentrates via shear rate-temperature-concentration superpositioning. *Journal of Food Science and Technology*, 55(3), 1207–1213. <https://doi.org/10.1007/s13197-017-3024-7>
- Ahmed, J. (2017). “Chapter 9 - Time-temperature superposition principle and its application to biopolymer and food rheology,” 33
- Allison, S. D., Chang, B., Randolph, T. W., & Carpenter, J. F. (1999). Hydrogen bonding between sugar and protein is responsible for inhibition of dehydration-induced protein unfolding. *Archives of Biochemistry and Biophysics*, 365(2), 289–298. <https://doi.org/10.1006/abbi.1999.1175>
- Anandharamakrishnan, C., RIELLY, C. D., & STAPLEY, A. G. F. (2008). Loss of solubility of α -lactalbumin and β -lactoglobulin during the spray drying of whey proteins. *LWT - Food Science and Technology*, 41(2), 270–277. <https://doi.org/10.1016/j.lwt.2007.03.004>
- Anandharamakrishnan, C., RIELLY, C. D., & STAPLEY, A. G. F. (2007). Effects of process variables on the denaturation of whey proteins during spray drying. *Drying Technology*, 25(5), 799–807. <https://doi.org/10.1080/07373930701370175>
- Anderson, A. D., Daubert, C. R., & Farkas, B. E. (2002). Rheological characterization of skim milk stabilized with carrageenan at high temperatures. *Journal of Food Science*, 67(2), 649–652. <https://doi.org/10.1111/j.1365-2621.2002.tb10654.x>
- AOAC. (2005). *Official methods of analysis* (18th ed.). Association of official analytical chemists.
- Baldwin, A. J. (2010). Insolubility of milk powder products – a minireview. *Dairy Science & Technology*, 90(2–3), 169–179. <https://doi.org/10.1051/dst/2009056>
- Da Silva, V. B., & da Costa, M. P. (2017). Rheology applied to dairy products. *Open Access*, 1(2), 2.
- Dahbi, L., Alexander, M., Trappe, V., Dhont, J. K. G., & Schurtenberger, P. (2010). Rheology and structural arrest of casein suspensions. *Journal of Colloid and Interface Science*, 342(2), 564–570. <https://doi.org/10.1016/j.jcis.2009.10.042>
- Dak, M., Verma, R. C., & Jaaffrey, S. N. A. (2007). Effect of temperature and concentration on rheological properties of ‘kesar’ mango juice. *Journal of Food Engineering*, 80(4), 1011–1015. <https://doi.org/10.1016/j.jfoodeng.2006.08.011>
- Dak, M., Verma, R. C., & Jaaffrey, S. N. A. (2008). Rheological properties of tomato concentrate. *International Journal of Food Engineering*, 4(7). <https://doi.org/10.2202/1556-3758.1470>
- Deswal, A., Deora, N. S., & Mishra, H. N. (2014). Effect of concentration and temperature on the rheological properties of oat milk. *Food and Bioprocess Technology*, 7(8), 2451–2459. <https://doi.org/10.1007/s11947-014-1332-8>
- Foroutan, A., Guo, A. C., Vazquez-Fresno, R., Lipfert, M., Zhang, L., Zheng, J., Badran, H., et al. (2019). Chemical composition of commercial cow’s milk. *Journal of Agricultural and Food Chemistry*, 67(17), 4897–4914. <https://doi.org/10.1021/acs.jafc.9b00204>
- Hadley, W. (2016). Ggplot2: Elegant graphics for data analysis. Springer-Verlag New York. <https://ggplot2.tidyverse.org>
- Harper, J. C., & Sahrigi, A. F. (1965). Viscometric behavior of tomato concentrates. *Journal of Food Science*, 30(3), 470–476. <https://doi.org/10.1111/j.1365-2621.1965.tb01788.x>
- Havea, P. (2006). Protein interactions in milk protein concentrate powders. *International Dairy Journal*, 16(5), 415–422. <https://doi.org/10.1016/j.idairyj.2005.06.005>
- Houssard, C., Maxime, D., Pouliot, Y., & Margni, M. (2021). Allocation is not enough! A system boundaries expansion approach to account for production and consumption synergies: The environmental footprint of Greek yogurt. *Journal of Cleaner Production*, 283(February), 124607. <https://doi.org/10.1016/j.jclepro.2020.124607>
- Joyce, A. M., Brodtkorb, A., Kelly, A. L., & O’Mahony, J. A. (2017). Separation of the effects of denaturation and aggregation on whey-casein protein interactions during the manufacture of a model infant formula. *Dairy Science & Technology*, 96(6), 787–806. <https://doi.org/10.1007/s13594-016-0303-4>
- Kaya, A., & Sozer, N. (2005). Rheological behaviour of sour pomegranate juice concentrates (Punica granatum L.). *International Journal of Food Science and Technology*, 40(2), 223–227. <https://doi.org/10.1111/j.1365-2621.2004.00897.x>

- Kobus, Z., Nadulski, R., Wilczyński, K., Starek, A., Zawislak, K., Rydzak, L., & Andrejko, D. (2019). Modeling of rheological properties of cloudy apple juice using master curve. *CyTA - Journal of Food*, *17*(1), 648–655. <https://doi.org/10.1080/19476337.2019.1630484>
- Market Data Forecast. (2022). “Lactose free market - Global industry analysis, size, share, growth, trends, and forecast 2021 – 2026.” Mareket Data Forecast. January 2022. <https://www.marketdataforecast.com/market-reports/lactose-free-market>.
- Prestrelski, S. J., Tedeschi, N., Arakawa, T., & Carpenter, J. F. (1993). Dehydration-induced conformational transitions in proteins and their inhibition by stabilizers. *Biophysical Journal*, *65*(2), 661–671. [https://doi.org/10.1016/S0006-3495\(93\)81120-2](https://doi.org/10.1016/S0006-3495(93)81120-2)
- Quek, M. C., Chin, N. L., & Yusof, Y. A. (2013). Modelling of rheological behaviour of soursop juice concentrates using shear rate–temperature–concentration superposition. *Journal of Food Engineering*, *118*(4), 380–386. <https://doi.org/10.1016/j.jfoodeng.2013.04.025>
- Rao, M. A. (2007). *Rheology of fluid and semisolid foods: Principles and applications*. 2nd ed. Food Engineering Series. New York: Springer.
- Rao, M. A., Bourne, M. C., & Cooley, H. J. (1981). Flow properties of tomato concentrates. *Journal of Texture Studies*, *12*(4), 521–538. <https://doi.org/10.1111/j.1745-4603.1981.tb00265.x>
- Sánchez, J., Hernández, E., Auleda, J. M., & Raventós, M. (2011). Review: Freeze concentration technology applied to dairy products. *Food Science and Technology International*, *17*(1), 5–13. <https://doi.org/10.1177/1082013210382479>
- Simuang, J., Chiewchan, N., & Tansakul, A. (2004). Effects of fat content and temperature on the apparent viscosity of coconut milk. *Journal of Food Engineering*, *64*(2), 193–197. <https://doi.org/10.1016/j.jfoodeng.2003.09.032>
- Solanki, G., & Rizvi, S. S. H. (2001). Physico-Chemical properties of skim milk retentates from microfiltration. *Journal of Dairy Science*, *84*(11), 2381–2391. [https://doi.org/10.3168/jds.S0022-0302\(01\)74687-5](https://doi.org/10.3168/jds.S0022-0302(01)74687-5)
- Stewart, Hayden. (2018). “Examining the decline in U.S. per capita consumption of fluid cow’s milk, 2003–18,” 42.
- Torres, J. K., Ferreira, R. S., Tavares, G. M., Fernandes, A., de Carvalho, R., Costa, G. B., Rocha, C. E., de Almeida, M., Almeida, R., Cappa, L. F., de Oliveira, P., & Schuck, and Ítalo Tuler Perrone. (2017). Technological aspects of lactose-hydrolyzed milk powder. *Food Research International*, *101*(November), 45–53. <https://doi.org/10.1016/j.foodres.2017.08.043>
- Ugidos-Rodríguez, S., Matallana-González, M. C., & Sánchez-Mata, M. C. (2018). Lactose malabsorption and intolerance: A review. *Food & Function*, *9*(8), 4056–4068. <https://doi.org/10.1039/C8FO00555A>
- Van Gorp, M., & Palmen, J. (1998). Time-temperature superposition for polymeric blends. 4.
- Vélez-Ruiz, J. F., & Barbosa-Cánovas, G. V. (1997). Effects of concentration and temperature on the rheology of concentrated milk. *Transactions of the ASAE*, *40*(4), 1113–1118. <https://doi.org/10.13031/2013.21328>
- Vélez-Ruiz, J. F., & Barbosa-Cánovas, G. V. (1998). Rheological properties of concentrated milk as a function of concentration, temperature and storage time. *Journal of Food Engineering*, *35*(2), 177–190. [https://doi.org/10.1016/S0260-8774\(98\)00019-3](https://doi.org/10.1016/S0260-8774(98)00019-3)
- Warncke, M., & Kulozik, U. (2020). Impact of temperature and high pressure homogenization on the solubility and rheological behavior of reconstituted dairy powders of different composition. *Powder Technology*, *376*(October), 285–295. <https://doi.org/10.1016/j.powtec.2020.08.039>
- Zhang, Y., An, Z., Bai, H., Li, Qi., & Guo, Z. (2015). Characterization and measurement of apparent viscosity of solid particles in fixed beds under high temperature. *Powder Technology*, *284*(November), 279–288. <https://doi.org/10.1016/j.powtec.2015.06.069>
- Zhao, X., Cheng, M., Zhang, X., Li, X., Chen, Di., Qin, Y., Wang, J., & Wang, C. (2020). The effect of heat treatment on the microstructure and functional properties of whey protein from goat milk. *Journal of Dairy Science*, *103*(2), 1289–1302. <https://doi.org/10.3168/jds.2019-17221>

Publisher's Note Springer Nature remains neutral with regard to jurisdictional claims in published maps and institutional affiliations.

Springer Nature or its licensor (e.g. a society or other partner) holds exclusive rights to this article under a publishing agreement with the author(s) or other rightsholder(s); author self-archiving of the accepted manuscript version of this article is solely governed by the terms of such publishing agreement and applicable law.